PHYSICAL REVIEW E **93**, 010201(R) (2016)

Control and generation of drifting patterns by asymmetrical Fourier filtering

E. Louvergneaux,[1,*] V. Odent,[1,†] S. Coulibaly,[1] U. Bortolozzo,[2] and S. Residori[2]
[1]*Univ. Lille, CNRS, UMR 8523–PhLAM–Physique des Lasers Atomes et Molécules, F-59000 Lille, France*
[2]*INLN, Université de Nice-Sophia Antipolis, CNRS, 1361 route des Lucioles, 06560 Sophia Antipolis, France*
(Received 28 May 2015; revised manuscript received 26 October 2015; published 7 January 2016)

We report the theoretical and experimental demonstration of one-dimensional drifting patterns generated by asymmetrical Fourier filtering in the transverse plane of an optical feedback system with a Kerr type nonlinearity. We show, with good agreement between our theoretical (analytics and numerics) calculations and experimental observations that at the primary instability threshold the group velocity is always different from zero. Consequently, the system is convective at this threshold, then exhibits drifting patterns.

DOI: 10.1103/PhysRevE.93.010201

Nonlinear pattern-forming systems are known to exist in nature in a large variety of physical contexts, such as hydrodynamics, optics, granular matter, plasma waves, soft matter, biology, and atom physics [1–4]. Controlling pattern formation is one of the most attractive topics in this framework, particularly in optics, where the ability to select and manage the spatial and temporal frequencies leading to the buildup of the optical field can have important consequences, not only for the fundamental point of view but also for practical applications. In this context drifting patterns have been reported for different nonlinear optical systems and based on various mechanisms. For instance, drifting mode instabilities have been observed by introducing nonlocality in the optical feedback loop [5] or by imposing an external parameter gradient [6], traveling waves have been obtained by frequency detuning in a nonlinear cavity [7], and advection of localized structures has been produced by a mirror tilt in the feedback loop [8]. Drifting rolls have also been reported in thermally driven convection in an inclined layer [9] and in electroconvection due to a slow lateral drift of charges in nematic liquid crystals [10]. Whatever the way to generate the patterns, their control requires one to handle their spatial frequency spectrum. For this purpose, Fourier filtering is a well-known technique. Indeed, spatial frequencies can easily be handled in optics since the Fourier transform of an input beam coincides with its field distribution in the focal plane of a lens [11]. Such a method has been used, for example, to achieve the control of spatiotemporal patterns in a nonlinear optical system [12], for optical pattern stabilization [13,14], control of turbulence [15], and spectrometry [16].

In this Rapid Communication, we propose asymmetrical Fourier filtering as a novel method to generate and control drifting patterns in an optical Kerr-like feedback system. From the point of view of linear systems, Fourier filtering is a well-known technique that finds multiple applications, such as FM radio selection [17], audio Digital Signal Processor (DSP)/equalizer [18], and noise reduction on images [19], to mention a few. To do so, selected temporal or spatial frequencies are removed or diminished symmetrically with respect to the zero frequency (dc). The question that arises is what happens if the filtering applies asymmetrically with respect to this later dc component, that is, to either only positive or negative frequencies, and how this kind of filtering in the spatial frequency spectrum can affect the patterns emerging in a nonlinear system. Here, we address the concept of positive and negative frequencies in spatial optics and show that asymmetrical Fourier filtering can be implemented leading to drifting patterns. Experimentally, we achieve the asymmetrical Fourier filtering on a one-dimensional liquid crystal Kerr-like nonlinear medium submitted to optical feedback. We show that the addition of the asymmetrical Fourier filtering turns the pattern-forming system into a convective one, that is, a system where transverse patterns are propagative [20,21]. We demonstrate that depending on the spatial frequency cutoff and on the value of the optical pump intensity, it is possible to control the phase velocity of the drifting pattern while keeping its wavelength almost constant. Analytical expressions of group and phase velocities at primary threshold of instability are derived for the ideal uniform extended system. Experimental phase velocities and instability thresholds measured for the one-dimensional system agree well with the analytical and numerical predictions. It is worth noting that, by making appropriate analogies, similar methods could be applied in other pattern-forming systems, opening the possibility to use the same mechanism for controlling spatiotemporal structures in different contexts.

The studied system is the well-known Kerr medium with optical feedback, as originally introduced by Akhmanov *et al.* [22] and later adapted by Firth and d' Alessandro [23,24] for pattern generation. Here, the Kerr medium is a liquid crystal cell and the model is slightly modified to add a Fourier filtering in the feedback loop [Fig. 1(a)]. The Kerr equation that captures most of the relevant dynamics of the liquid crystal refractive index n reads

$$\tau \frac{\partial n}{\partial t} - l_d^2 \frac{\partial^2 n}{\partial x^2} + n = |F|^2 + |B|^2 + \sqrt{\epsilon}\xi(x,t), \qquad (1)$$

where $n(x,t)$ stands for the refractive index of the nonlinear nematic LC layer, and t and x are the time and space variables scaled with respect to the relaxation time τ and the diffusion length l_d. $\xi(x,t)$ describes a Gaussian stochastic process of zero mean and correlation $\langle \xi(x,t)\xi(x',t')\rangle = \langle \delta(x-x')\delta(t-t')\rangle$. The level of noise is controlled by the parameter ϵ, which is purely phenomenological. The small thickness of the Kerr medium allows neglecting light diffraction along the sample. F and B are the dimensionless

*eric.louvergneaux@univ-lille1.fr; http://www.phlam.univ-lille1.fr/spip.php?article66
†vincent.odent@univ-lille1.fr

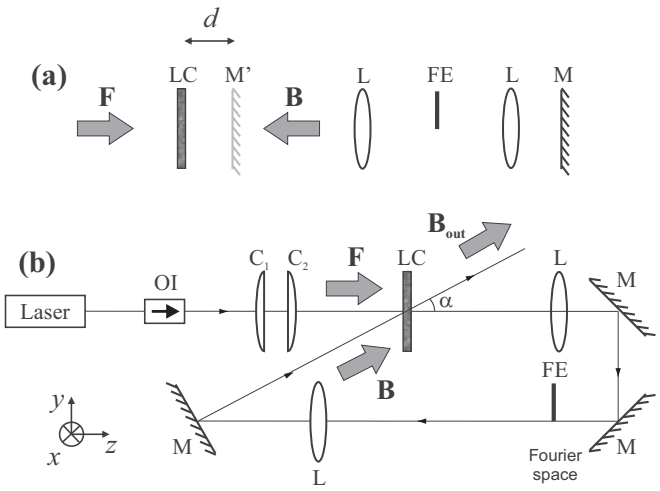

FIG. 1. (a) Schematic representation of the Kerr feedback system with asymmetric Fourier filtering. (b) Experimental setup. OI, optical isolator; C_1 and C_2 are cylindrical lenses; LC, liquid crystal slice; L lenses of focal length f; BS, beam splitter; M are the mirrors; FE, filtering element in the Fourier space. F and B are, respectively, the forward and the backward fields. M is the feedback mirror and M' its image through the two L lenses ($4f$ arrangement). d is the *equivalent optical* feedback distance between M' and LC.

forward and backward fields, respectively [24]. Equation (1) must be completed by the two following equations describing the propagation through the sample and over the feedback loop, respectively:

$$\frac{\partial F}{\partial z} = i\chi n F \quad \text{and} \quad \frac{\partial F}{\partial z} = \frac{-i}{2k_0}\nabla_\perp^2 F, \tag{2}$$

where χ parametrizes the Kerr effect (positive for a focusing medium, $d > 0$) and k_0 is the optical wave number. The length of the optical feedback loop is $2d$ [Fig. 1(a)]. The transverse profile of the forward field is accounted for by the expression $F(x) = F_0 g(x)$, with $g(x) = e^{-(x/w)^2}$ describing a Gaussian pump of radius w and $g(x) = 1$ corresponding to the uniform (plane wave) case.

In order to simplify mathematics, but without loss of generality, we have considered the plane wave approximation in our calculations $g[(x) = 1]$ and assume that our system is deterministic ($\epsilon = 0$). Next, the asymmetrical filtering is applied in the Fourier space during the propagation of the backward field B by introducing a Heaviside function. Then, after the propagation inside the feedback loop the backward field is obtained as follows:

$$B = F\sqrt{R}\, e^{id\partial^2/k_0\partial x^2}(e^{i\chi n}) \otimes \int_{-\infty}^{+\infty} \tilde{H}(k - k_d) e^{ikx} dk, \tag{3}$$

where R stands for the intensity reflection coefficient, k_d the value of the filtering wave-number cutoff in the Fourier plane, $\tilde{H}$ the Heaviside function, and $\otimes$ the convolution product. Setting $\frac{\partial}{\partial t} = 0$ and $\frac{\partial^2}{\partial x^2} = 0$ in Eq. (1), we found that the homogeneous steady state (HSS) of the refractive index can be written as $n_{SH} = I_0[1 + RH^2(-k_d)]$ [24], where $I_0 = |F|^2$. The linear stability analysis of this HSS with respect to perturbations of the form $\delta n \sim \exp(i\Omega t - ikx)$, with $\Omega = \Omega^r + i\Omega^i$ and $k = k^r + ik^i$, leads to the following equations:

$$\begin{aligned} \Omega^r &= \frac{\mu\tilde{H}(-k_d)}{\tau}\cos\left(\frac{dk^2}{k_0}\right)[\tilde{H}^+ - \tilde{H}^-], \\ \Omega^i &= \frac{-\mu\tilde{H}(-k_d)}{\tau}\sin\left(\frac{dk^2}{k_0}\right)[\tilde{H}^+ + \tilde{H}^-] + \frac{l_d^2k^2 + 1}{\tau}, \end{aligned} \tag{4}$$

which correspond to the real and imaginary parts of the dispersion relations, respectively. Here we have set $\tilde{H}^+ = \tilde{H}(k - k_d)$, $\tilde{H}^- = \tilde{H}(-k - k_d)$, and $\mu = RI_0|\chi|$. Next, the onset of the instability I_c and the associated wave number k_c are calculated by means of the following system of equations [25]:

$$\Omega^i(k_c, \mu_c) = 0, \quad \partial\Omega^i/\partial k^r|_{k_c} = 0, \quad \text{and} \quad k^i = 0. \tag{5}$$

Solving this system, we have obtained

$$I_c = \frac{1 + k_c^2 l_d^2}{\chi R\tilde{H}(-k_d)\sin\left(\frac{dk_c^2}{k_0}\right)(\tilde{H}_c^+ + \tilde{H}_c^-)} \tag{6}$$

with $\tilde{H}_c^+ = \tilde{H}(k_c - k_d)$, $\tilde{H}_c^- = \tilde{H}(-k_c - k_d)$. Notice that this expression of the instability threshold has to be in contrast to those obtained without any filtering, given by [26]:

$$I_{c_0} = \frac{1 + k_{c0}^2 l_d^2}{2\chi R\,\sin\left(\frac{dk_{c0}^2}{k_0}\right)}, \tag{7}$$

k_{c0} being the corresponding wave number. As for the instability threshold, we have obtained that the filtering impacts also the group and phase velocity. Indeed, considering $v_g = \partial\Omega^r/\partial k^r$ and $v_\varphi = \Omega^r/k^r$ the group velocity and phase velocity, respectively, from (4) we have

$$\begin{aligned} v_g = &-2\mu_c\tilde{H}(-k_d)\sin\left(\frac{dk_c^2}{k_0}\right)[\tilde{H}_c^+ - \tilde{H}_c^-] \\ &+ \mu_c\tilde{H}(-k_d)\cos\left(\frac{dk_c^2}{k_0}\right)[\delta(k_c - k_d) + \delta(k_c + k_d)], \end{aligned} \tag{8}$$

and

$$v_\varphi = \frac{\mu_c\tilde{H}(-k_d)}{k_c}\cos\left(\frac{dk_c^2}{k_0}\right)[\tilde{H}_c^+ - \tilde{H}_c^-]. \tag{9}$$

Equation (8) demonstrates that, depending on the cutoff wave number k_d, the group velocity v_g have always a nonzero value at the primary instability threshold when the filtering really affects initial wave numbers, that is, if $k_d \leqslant k_{c_0}$. This implies that the filtered system displays convective instabilities ($v_g \neq 0$) at the primary instability threshold, coupled with the emergence of drifting patterns ($v_\varphi \neq 0$) [27]. Indeed, convective systems depict propagative patterns [20,21,26]. Thus, drifting patterns are always generated in the asymmetrical filtered system, except for very particular values of the parameters that cancel the phase velocity, but never the group velocity. Numerical simulations in the deterministic uniform case ($g = 1$, $\epsilon = 0$) confirm these analytical predictions. Table I shows the results obtained by taking into account the experimental features, namely, a large aspect ratio Gaussian profile for the pump beam, $g(x) = e^{-(x/w)^2}$, and noise, $\epsilon \neq 0$. It can be noted that including the noise and the Gaussian profile practically does

TABLE I. Comparison of the values of phase velocity (v_φ), pump intensity I_c, and wave number k_c at the primary instability threshold for analytical predictions, and three different numerical simulations. Namely, a uniform deterministic system, a uniform stochastic system, and a Gaussian stochastic system (experimental one). Parameters for simulations are $k_d = 0.11k_{c_0}$, $d = 8$ mm, $R_{eq} = 68\%$, $v_g = 33.4\ \mu\mathrm{m\,s}^{-1}$.

	v_φ (μm/s)	I_c	k_c (mm^{-1})
Analytical predictions and ($g = 1, \epsilon = 0$) simulations	−1.40	1.79	46.26
($g = 1, \epsilon \neq 0$) simulations	−1.46	1.76	45.99
($g = e^{-(x/w)^2}, \epsilon \neq 0$) simulations	−1.46	1.76	46.17

not affect the values of the phase velocity v_φ, the primary instability threshold μ_c, and the associated wave number k_c. Therefore, the predicted dynamics survives even in the experimental conditions. However, the presence of noise does not allow the measurement of the group velocity because noise acts as a continuous microscopic source of perturbations and the velocity of a single local perturbation cannot be accessed. From the dynamical point of view, noise transforms convective patterns into noise-sustained structures [26,28].

Departing from above the primary threshold, patterns are always found propagative, that is, $v_\varphi \neq 0$, except for very specific values of k_d that cancel v_φ but not v_g, indicating that the system is always convective away from the convective threshold. Indeed, we have checked that $v_g \neq 0$. A typical evolution of the phase velocity with increasing pump intensity is depicted in Fig. 2(a) for $k_d = 0.94k_{c_0}$ (for this particular value of the cutoff the phase velocity is null at convective threshold). The phase velocity v_φ continuously changes from negative to positive values [Fig. 2(a)]. In the same time, the wavelength of the associated propagative pattern does not vary significantly. For a range of pump intensities up to two times the primary threshold, the relative change of the pattern wave number remains well below 5% [Fig. 2(b)]. Thus, the drifting velocity of the transverse pattern can be continuously tuned with an "almost" constant wavelength. Corresponding simulations are displayed in Figs. 3(d)–3(f). The spatiotemporal diagrams demonstrate that the drift velocity of the pattern is driven from negative, zero, and then positive values by increasing the pump intensity I. This evidence opens the possibility to control the drift velocity of a spatial structure in pattern-forming systems.

Corresponding experiments are carried out on the setup shown in Fig. 1(b). It essentially consists of a nematic liquid crystal (LC) layer submitted to an optical feedback. The main difference with previous experiments is that the feedback loop is not achieved by using a single mirror but with a "ring" configuration consisting of three aligned mirrors. The reason for the choice of the ring geometry is that the 4f lens imaging system inserted in the feedback loop [29–31] only allows for symmetrical Fourier filtering when using the single mirror configuration [Fig. 1(a)]. Using a ring configuration allows us to perform asymmetrical Fourier filtering in the focal plane of the first lens of the feedback loop. A resulting effect is to introduce a small angle α between the feedback beam B and

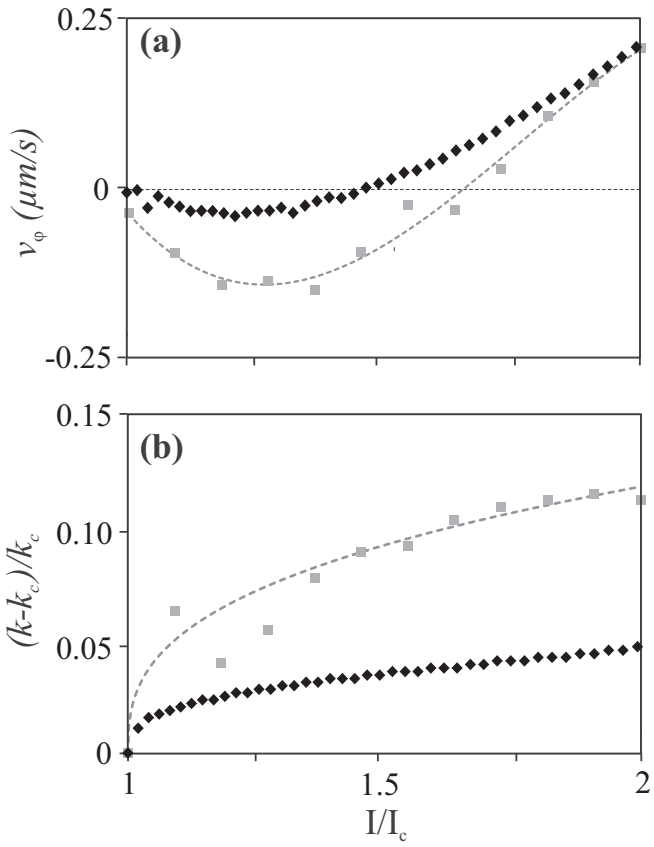

FIG. 2. Influence of the input pump intensity on the evolutions of (a) the phase velocity and (b) the wave number above the primary instability threshold for $k_d(\mathrm{num}) = 0.94k_{c_0}$ and $k_d(\mathrm{exp}) = 0.95k_{c_0}$. ♦, stochastic numerical simulations; ■, experimental results. Parameters are $I_c = 98\ \mathrm{W/cm^2}$, $\epsilon = 0.1$, $w = 2200\ \mu$m, $d = 8$ mm, $R_{eq} = 68\%$. The dashed lines are empirical fits only drawn for a better reading of the experimental data tendency.

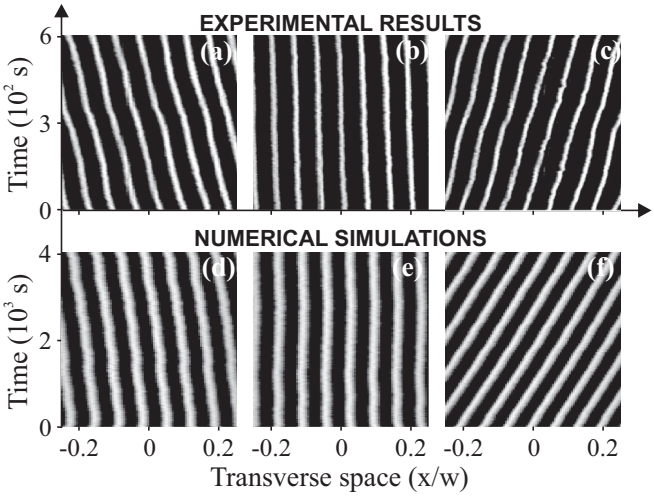

FIG. 3. (a)–(c) Experimental and (d)–(f) numerical dynamical evolutions of the transverse cross section of the near-field transverse pattern versus pumping intensity. (a), (d) $I = 1.36\ I_c$; (b), (e) $I = 1.55\ I_c$; (c), (f) $I = 1.90\ I_c$, $I_c = 98\ \mathrm{W/cm^2}$. $k_d(\mathrm{num}) = 0.94k_{c_0}$, $k_d(\mathrm{exp}) = 0.95 \pm 0.06k_{c_0}$. $d = 8$ mm, $w = 2200\ \mu$m, $R_{eq} = 68\%$, $\chi = 1, \epsilon = 0.1$.

the incoming beam F. In our case, $\alpha = 15^\circ$. This angle corresponds to optical interference fringes ($\sim 2\ \mu$m) that are erased by the nematic liquid crystal diffusion whose characteristic length is $l_d = 10\ \mu$m. The equivalent optical feedback distance is $d = 8$ mm [Fig. 1(a)] [32,33]. The nonlinear medium is a 50-μm-thick layer of E_7 LC homeotropically anchored. The beam is delivered by a monomode frequency doubled Nd^{3+}:YVO_4 laser ($\lambda_0 = 532$ nm) which is shaped by means of two cylindrical telescopes, C_1 and C_2, in order to achieve a transverse quasi-one-dimensional (1D) pumping following the x axis (beam waist $w_x \times w_y \approx 2200\ \mu\text{m} \times 350\ \mu\text{m}$). The backward beam B_{out} [Fig. 1(b)] is monitored after its second passage through the LC layer.

Without any spatial filtering in the Fourier space, we observe a regular and stationary pattern at the primary threshold for the transverse instability $I_{c_0} = 78\ \text{W/cm}^2$. The pattern wave number is $k_{c_0} = 48.3\ \text{mm}^{-1}$ [34]. Then, we apply the filtering element by translating a half-cutting edge in the focal plane of the first lens of the $4f$ lens arrangement in the feedback loop [FE in Fig. 1(a)]. In order to check the ability of the asymmetrical Fourier filtering in generating and controlling the drifting patterns, we performed our experiments by using the same cutoff as for the numerical simulations, $k_d = (0.95 \pm 0.06)k_{c_0}$. For this cutoff the drift velocity can be tuned continuously with an almost constant wavelength. We record the pattern near-field dynamics for increasing the pump intensity [Figs. 3(a)–3(c)]. Then, we show that increasing the pump value above the primary threshold allows one to continuously tune the phase velocity. This is reported in Fig. 2(a). We want to emphasize that the global evolution of the experimental drift velocity follows qualitatively well the one from the stochastic numerical predictions. In parallel, the experimental pattern wave number remains within 10% of its relative change for a pump intensity ranging up to two times the primary threshold value. This experimentally confirms the predictions, evidencing the control of the drift velocity of a spatial structure while keeping its wave number almost unchanged.

To summarize, we demonstrate that the application of an asymmetrical Fourier filtering in the feedback loop of a Kerr system changes it to be convective, that is, transverse patterns become propagative. We show that the induced noise-sustained and absolute patterns are always propagative above the convective threshold. We demonstrate that we can manage the drift velocity of the transverse patterns while keeping its wavelength "almost" constant. The data show very good agreement between analytical predictions, numerical simulations, and experimental results. The asymmetrical Fourier filtering method could also be applied in other pattern-forming systems and appears to be a viable way to control and manage pattern formation. For example, this method could be applied for the control of charge waves or for enhancing the performances of scanning/transport mechanisms, particularly, with interest for biological applications and photonic devices.

The authors thank H. Louis for fruitful discussions. V.O. acknowledges the support of the "Région Nord-Pas-de-Calais." This work has been partially supported by the Centre National de la Recherche Scientifique (CNRS), the Ministry of Higher Education and Research, the Nord-Pas de Calais Regional Council, and European Regional Development Fund (ERDF) through the Contrat de Projets état-Région (CPER) 2007–2013, as well as by the Agence Nationale de la Recherche through the LABEX CEMPI project (ANR-11-LABX-0007).

[1] M. Cross and P. Hohenberg, Rev. Mod. Phys. **65**, 851 (1993).
[2] S. Chandrasekhar, *Hydrodynamic and Hydromagnetic Stability* (Clarendon, Oxford, 1961).
[3] J. D. Murray, *Mathematical Biology* (Springer-Verlag, Berlin, 1989).
[4] *Dissipative Solitons: From Optics to Biology and Medicine*, edited by N. Akhmediev and A. Ankiewicz, Lecture Notes in Physics Vol. 751 (Springer, Berlin/Heidelberg, 2008).
[5] P. L. Ramazza, P. Bigazzi, E. Pampaloni, S. Residori, and F. T. Arecchi, Phys. Rev. E **52**, 5524 (1995).
[6] C. Cleff, B. Gütlich, and C. Denz, Phys. Rev. Lett. **100**, 233902 (2008).
[7] U. Bortolozzo, P. Villoresi, and P. L. Ramazza, Phys. Rev. Lett. **87**, 274102 (2001).
[8] F. Haudin, R. G. Rojas, U. Bortolozzo, M. G. Clerc, and S. Residori, Phys. Rev. Lett. **106**, 063901 (2011).
[9] K. E. Daniels, B. B. Plapp, and E. Bodenschatz, Phys. Rev. Lett. **84**, 5320 (2000).
[10] A. Joets and R. Ribotta, Phys. Rev. Lett. **60**, 2164 (1988).
[11] J. W. Goodman, *Introduction to Fourier Optics*, 3rd rev. ed. (Roberts and Company, Greenwood Village, CO, 2005).
[12] L. Pastur, L. Gostiaux, U. Bortolozzo, S. Boccaletti, and P. Ramazza, Phys. Rev. Lett. **93**, 063902 (2004).
[13] S. Jensen, M. Schwab, and C. Denz, Phys. Rev. Lett. **81**, 1614 (1998).
[14] A. Mamaev and M. Saffman, Phys. Rev. Lett. **80**, 3499 (1998).
[15] D. Hochheiser, J. V. Moloney, and J. Lega, Phys. Rev. A **55**, R4011 (1997).
[16] E. Rohner and M. J. O. Strutt, Rev. Sci. Instrum. **28**, 1074 (1957).
[17] G. J. King, *FM Radio Servicing Handbook*, 2nd ed. (Newnes-Butterworth, London, 1970).
[18] R. W. Schafer and A. V. Oppenheim, *Discrete-Time Signal Processing*, 3rd ed. (Prentice Hall, Englewood Cliffs, NJ, 2009).
[19] D. Van De Ville, M. Nachtegael, D. Van der Weken, E. E. Kerre, W. Philips, and I. Lemahieu, IEEE Trans. Fuzzy Syst. **11**, 429 (2003).
[20] R. J. Briggs, *Electron-Stream Interaction with Plasmas* (MIT Press, Cambridge, MA, 1964).
[21] P. Huerre and P. Monkewitz, Annu. Rev. Fluid Mech. **22**, 473 (1990).
[22] S. A. Akhmanov, M. A. Vorontsov, and V. Yu. Ivanov, Pis'ma Zh. Eksp. Teor. Fiz. **47**, 611 (1988) [JETP Lett. **47**, 707 (1988)].
[23] W. Firth, J. Mod. Opt. **37**, 151 (1990).
[24] G. D'Alessandro and W. J. Firth, Phys. Rev. A **46**, 537 (1992).
[25] C. Bender and S. Orszag, *Advanced Mathematical Methods for Scientists and Engineers* (McGraw-Hill, New York, 1978).

[26] E. Louvergneaux, C. Szwaj, G. Agez, P. Glorieux, and M. Taki, Phys. Rev. Lett. **92**, 043901 (2004).

[27] One can mention that fortunately, v_φ is always null when v_g is null, which is a direct consequence of an absolute system.

[28] M. Santagiustina, P. Colet, M. San Miguel, and D. Walgraef, Phys. Rev. Lett. **79**, 3633 (1997).

[29] G. Agez, C. Szwaj, and E. Louvergneaux, Phys. Rev. A **66**, 063805 (2002).

[30] P. Kockaert, P. Tassin, G. Van der Sande, I. Veretennicoff, and M. Tlidi, Phys. Rev. A **74**, 033822 (2006).

[31] P. Tassin, L. Gelens, J. Danckaert, I. Veretennicoff, P. Kockaert, and M. Tlidi, Chaos **17**, 037116 (2007).

[32] P. Kockaert, J. Opt. Soc. Am. B **26**, 1994 (2009).

[33] V. Odent, M. Tlidi, M. G. Clerc, P. Glorieux, and E. Louvergneaux, Phys. Rev. A **90**, 011806 (2014).

[34] E. Louvergneaux, Phys. Rev. Lett. **87**, 244501 (2001).